JBIC Journal of Biological Inorganic Chemistry
https://doi.org/10.1007/s00775-020-01755-6

ORIGINAL PAPER

Cytotoxicity, alpha-glucosidase inhibition and molecular docking studies of hydroxamic acid chromium(III) complexes

Latifah Robbaniyyah Hassan[1] · El Hassane Anouar[2] · Hadariah Bahron[1,3] · Faiezah Abdullah[4] · Amalina Mohd Tajuddin[1,5]

Received: 8 October 2019 / Accepted: 9 January 2020

Abstract

Hydroxamic acids [R(CO)N(OH)R'] are flexible compounds for organic and inorganic analyses due to their frailer structures compared to the carboxylic acid. The syntheses and characterization of benzohydroxamic acid (BHA), its CH_3–, OCH_3–, Cl– *para*-substituted derivatives and their Cr(III) complexes are reported herein. The metal complexes were synthesized by reacting the hydroxamic acids with chromium(III) chloride hexahydrate in 2:1 molar ratio. The compounds were characterized via melting point, elemental analysis, FTIR, ^{1}H and ^{13}C NMR, TGA, mass spectrometry, molar conductance and UV–Visible. Data analysis suggests that each complex has the Cr(III) center coordinated to the carbonyl and hydroxy oxygen atoms of the hydroxamic acids in bidentate *O,O* manner and two water molecules to form octahedral geometry. Non-electrolytic behavior of the complexes was shown through their low molar conductivity. Cytotoxicity study against HCT116 and alpha-glucosidase inhibition test revealed that all complexes have higher activity than their parent ligands. Molecular docking study shows that the docking of active complexes is thermodynamically favorable and the inhibition efficiency may depend on the types and the numbers of molecular interactions established in the corresponding stable conformers.

Keywords Benzohydroxamic acid · Chromium(III) · Cytotoxicity · Alpha-glucosidase · Molecular docking

Introduction

Hydroxamic acids, R(CO)N(OH)R', are a class of compounds that display many bioactive properties such as anticancer, antimalarial and antifungal [1]. These properties are caused by the ease of deprotonation to produce hydroxamate or hydroximate ions. The deprotonation renders these acids stable chelates for metals allowing them to interrupt enzyme activities [2-5]. They are also known to possess NO-releasing properties [6, 7] that are pharmacologically important, acting on smooth muscles as potential vasodilators and cardiac contractility regulators. Aromatic hydroxamic acids such as benzohydroxamic acid or salicylhydroxamic acid and their metal complexes have received a lot of attention due to their fascinating structures and myriad of bioactivities [8-10].

Chromium is one of the most common elements found on the earth crust and seawater. Like other transition metals, chromium has several oxidation states, the most common of which are metallic (Cr^0), trivalent (Cr^{3+}) and hexavalent (Cr^{6+}) chromium. Cr^{3+} is frequently found in food and well known as a dietary supplement [11], a crucial nutrient involved in the glucose tolerance factor (GTF) in maintaining regular carbohydrate and lipid metabolism. For example, chromium picolinate [$Cr(pic)_3$] supplement has been widely used to improve body's response to insulin in lowering blood sugar for people with type two diabetes [12]. Chromium

✉ El Hassane Anouar
anouarelhassane@yahoo.fr

✉ Amalina Mohd Tajuddin
amalina9487@uitm.edu.my

1 Faculty of Applied Sciences, Universiti Teknologi MARA, Shah Alam, 40450 Selangor, Malaysia

2 Department of Chemistry, College of Science and Humanities in Al-Kharj, Prince Sattam Bin Abdulaziz University, Al-Kharj 11942, Saudi Arabia

3 University of Malaya Centre for Ionic Liquid (UMCIL), Universiti Malaya, 50603 Kuala Lumpur, Malaysia

4 Centre of Foundation Studies, Universiti Teknologi MARA, Dengkil, 43800 Selangor, Malaysia

5 Atta-ur-Rahman Institute for Natural Product Discovery (AuRIns), Universiti Teknologi MARA, Level 9, FF3 Building, 42300 Puncak Alam, Selangor, Malaysia

Published online: 23 January 2020

metformin, [Cr(Met)] displayed beneficial effects on blood glucose and lipid metabolism for diabetic mice and reported to be safe where no damaging effects to cells were observed [13]. Chromium(III) glycinate complex supplementation has also been reported to improve blood glucose level and attenuates the copper to zinc ratio in tissues of rats with mild hyperglycaemia [14]. Additionally, *Cis*-$[Cr(C_2O_4)(pm)(OH_2)_2]^+$ cation has been tested as a specific sensing ion for the detection of hydrogen peroxide (H_2O_2) in HT22 hippocampal cells [15]. Being classified as a Reactive Oxygen Species (ROS), H_2O_2 is one of the most important mediators of oxidative stress sensing under pathological conditions, and it is also involved in cellular physiological activities as signal transduction molecules.

Computational chemistry approaches are considered powerful tools in supporting observed experimental results. Molecular docking is a computational tool that is largely used in structural molecular biology and computer-assisted drug design to find and predict the possible predominant binding modes between a docked ligand against a biological target protein. It has been successfully used to investigate the binding modes of many alpha-glucosidase inhibitors [16, 17]. There is an apparent lack of research on the effect of electron-withdrawing and electron-donating substituents on hydroxamic acids towards the cytotoxicity and antidiabetic activities.

In this paper, we report the synthesis and characterization of BHA and its methyl, methoxy and chloro- substituted derivatives namely CH_3–BHA, OCH_3–BHA, and Cl–BHA, respectively, and their Cr(III) metal complexes. All synthesized compounds were characterized through elemental analysis, FTIR, ^1H and ^{13}C NMR, TGA, mass spectrometry, molar conductance and UV–Visible. A preliminary cytotoxicity screening against HCT116 and alpha-glucosidase inhibition test of the hydroxamic acids and their chromium(III) complexes were carried out and reported herein.

Materials and methods

Chemicals and instruments

All the chemicals and reagents were purchased from Sigma Aldrich and Merck and used as received without further purification. Benzohydroxamic acid (BHA) is commercially available. The percent composition of the elements (CHN) for the compounds was determined by using Thermo Scientific Flash 2000 Elemental Analyzer with methionine as a standard. Melting points were determined in evacuated capillaries using Stuart SMP10 and were uncorrected. The infrared spectra (IR) were recorded on a Perkin-Elmer Model 1750X FTIR spectrophotometer in the range of 4000–400 cm^{-1} as KBr discs. The ^1H and ^{13}C NMR spectra were recorded on a Bruker Varian-600 MHz in deuterated DMSO using TMS as an internal standard. The mass spectrometric analysis was performed in an LC1200 Series Agilent Technologies controlled by Agilent Mass Hunter Workstation Acquisition (B.02.01). The separation was performed at 40 ºC with a ZORBAX Eclipse Plus C18 column 2.1 mm × 100 mm, 1.8 µm (Agilent Technologies SA, USA) with (A) 0.1% formic acid in water and (B) 0.1% formic acid in acetonitrile, over a gradient of 0 to 36 min with increasing percentage of B from 5 to 95%. The thermal decomposition behavior of the metal complexes was recorded using NETZSCH TG 209 F3 under the nitrogen atmosphere at a heating rate of 10 ºC min^{-1} from room temperature to 900 ºC. Magnetic moments of the complexes were measured using the Guoy method with water as calibrant on Sherwood Auto Magnetic Susceptibility Balance. Molar conductivity measurements of complexes were determined in dimethylsulfoxide (DMSO) and ethanol (10^{-3} M) at room temperature using a Mettler Toledo Inlab 730 conductivity meter. The UV–Visible spectra were obtained in ethanol in the 900–200 nm range using Perkin Elmer UV–Vis Lambda 35 spectrophotometer at room temperature.

Synthesis

Synthesis of methylbenzohydroxamic acid, CH_3–BHA

The synthesis of CH_3–BHA is represented in Scheme 1. Hydroxylamine hydrochloride (12 mmol, 0.9555 g) was added to a mixture solution of ethyl acetate and water containing sodium hydrogen carbonate ($NaHCO_3$). The mixture was stirred at room temperature. 4-Methylbenzoyl chloride was diluted with small amounts of ethyl acetate was added dropwise to the mixture. The mixture was stirred for 5 min at room temperature. The solvent was removed in *vacuo*

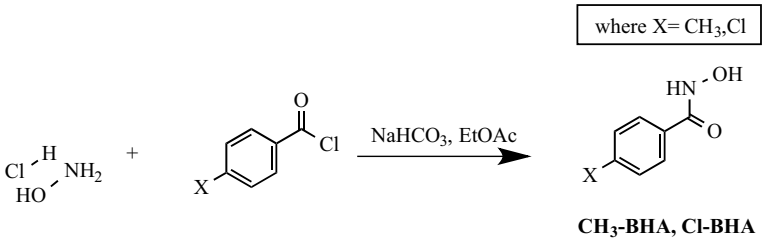

Scheme 1 Formation reaction of CH_3-BHA and Cl-BHA

to afford the pure product. Peach solid; yield, 100%; m.p. 152–154 ºC. Anal. Calcd. for $C_8H_9NO_2$ (151.20 $gmol^{-1}$): C, 63.56; H, 6.00; N, 9.27; Found: C, 62.71; H, 5.70; N, 9.00. IR (KBr, cm^{-1}): 3294 (N–H), 2759 (O–H), 1651 (C = O), 903 (N–O). ^{1}H NMR (600 MHz, ppm, DMSO): δ = 2.41 (3H, s, CH_3), 7.23–7.62 (2H, d, Ar–H), 7.62 (2H, d, Ar–H). ^{13}C NMR (600 MHz, ppm, DMSO): δ = 164.03, 140.61, 130.26, 128.76, 126.73, 20.89. MS (m/z): Calcd for CH_3–BHA: 152.20 $[M+H]^+$; Found: 152.07 $[M+H]^+$.

Synthesis of methoxybenzohydroxamic acid, [OCH_3–BHA]•H_2O

The synthesis of OCH_3–BHA is represented in Scheme 2. 10 mL of ethyl acetate was mixed with sodium bicarbonate (24 mmol, 2.1245 g) in 5 mL of ultra-pure water. Sodium bicarbonate solution was added to hydroxylamine hydrochloride (12 mmol, 0.9555 g) and stirred until dissolved at room temperature. A small amount of ethyl acetate was added to 4-methoxybenzoyl chloride (10 mmol, 1.7001 g) to dilute it before being added dropwise to the mixture. The mixture was stirred for 5 min at room temperature. The white precipitate was collected after the solvent was removed *in vacuo*. Peach solid; yield, 100%; m.p. 160–161 ºC. Anal. Calcd. for $C_8H_{11}NO_4$ (185.20 $gmol^{-1}$): C, 51.89; H, 5.99; N, 7.56; Found: C, 53.37; H, 4.91; N, 6.74. IR (KBr, cm^{-1}): 3285 (N–H), 2760 (O–H), 1669 (C = O), 902 (N–O). ^{1}H NMR (600 MHz, ppm, DMSO): δ = 3.80 (3 H, s, O–CH_3), 6.99 (2H, d, Ar–H), 7.74 (2H, d, Ar–H), 8.93 (1 H, s, O–H), 11.11 (1 H, s, N–H). ^{13}C NMR (600 MHz, ppm, DMSO): δ = 161.43, 131.29, 128.59, 113.77, 113.55, 55.20. MS (m/z): Calcd for OCH_3–BHA: 186.20 $[M+H]^+$; Found: 185.02 $[M+H]^+$.

Synthesis of chlorobenzohydroxamic acid, Cl–BHA

The synthesis of Cl–BHA is illustrated in Scheme 1. A mixture containing 10 mL ethyl acetate, 5 mL ultra-pure water and sodium bicarbonate (24 mmol, 2.0625 g) was mixed with hydroxylamine hydrochloride (12 mmol, 0.9767 g). The solution was stirred at room temperature until dissolved. A small amount of ethyl acetate was added dropwise to 4-chlorobenzoyl chloride (10 mmol, 1.8104 g) and stirred for 5 min at room temperature. The solvent was removed in *vacuo* and white solid was obtained before stored in a desiccator for further use. Peach solid; yield, 100%; m.p. 138–140 ºC. Anal. Calcd. for $C_7H_6ClNO_2$ (171.60 g mol^{-1}): C, 49.00; H, 3.52; N, 8.16; Found: C, 48.59; H, 3.38; N, 8.32. IR (KBr, cm^{-1}): 3292 (N–H), 2748 (O–H), 1650 (C = O), 900 (N–O). ^{1}H NMR (600 MHz, ppm, DMSO): δ = 7.54 (2 H, d, Ar–H), 7.80 (2 H, d, Ar – H), 9.16 (1 H, s, O–H), 11.36 (1H, s, N–H). ^{13}C NMR (600 MHz, ppm, DMSO): δ = 163.14, 135.91, 131.47, 128.76, 128.43. MS (m/z): Calcd for Cl–BHA: 172.60 $[M+H]^+$; Found: 172.02 $[M+H]^+$.

Synthesis of Cr(III) complexes

The reaction of metal salts with BHA and its derivatives, CH_3–BHA, OCH_3–BHA, and Cl–BHA in 1:2 molar ratio is represented by Scheme 3.

i) **Synthesis of Cr(III) benzohydroxamic acid, $[Cr(BHA)_2(H_2O)_2]\cdot H_2O$**

Chromium(III) chloride hexahydrate, $CrCl_3\cdot 6H_2O$ (1.63 mmol, 0.4343 g) was dissolved in a hot aqueous solution (10 mL) of BHA (3.26 mmol, 0.4471 g). The pH of the resulting solution was increased to 5.5 using 0.1 M NaOH solution, a green precipitate appeared. The obtained solid was filtered, washed with distilled water and dried in the air before stored in a desiccator. Muddy green solid; yield, 13.77%; m.p. > 280 ºC. Anal. Calcd. for $C_{14}H_{18}N_2O_7Cr$ (378.30 g mol^{-1}): C, 44.45; H, 4.80; N, 7.41; Found: C, 44.27; H, 4.10; N, 7.96. IR (KBr, cm^{-1}): 1602 (C = O), 917 (N–O), 489 (Cr–O). MS (m/z): Calcd for $[Cr(BHA)_2(H_2O)_2]\cdot H_2O$: 379.30 $[M+H]^+$; Found: 379.28 $[M+H]^+$. Molar conductance: 3.37 Ω^{-1} cm^2 mol^{-1}.

ii) **Synthesis of Cr(III) chlorobenzohydroxamic acid, $[Cr(Cl–BHA)_2(H_2O)_2]\cdot 2H_2O$**

Chromium(III) chloride hexahydrate, $CrCl_3\bullet 6H_2O$ (5 mmol, 0.6661 g) was dissolved in 10 mL of hot deionized water. Cl–BHA (10 mmol, 1.2431 g) was dissolved in 10 mL of hot absolute ethanol. Then, both of the solutions were mixed and stirred under nitrogen (N_2) gas for 3 h. The grey precipitate was obtained, filtered, washed with the warm water and air-dried. Finally, the product was collected and stored in a desiccator. Grey solid; yield, 13.19%; m.p. 188–189 ºC. Anal. Calcd. for $C_{14}H_{18}N_2O_8Cl_2Cr$ (465.20 g mol^{-1}): C, 36.15; H, 3.90; N, 6.02; Found: C, 36.52; H, 2.79; N, 6.22. IR (KBr, cm^{-1}): 3294 (N–H), 1651 (C = O), 900 (N–O), 476 (Cr–O). MS (m/z): Calcd for $[Cr(Cl–BHA)_2(H_2O)_2]\cdot 2H_2O$:

Scheme 2 Formation reaction of [OCH_3–BHA]•H_2O

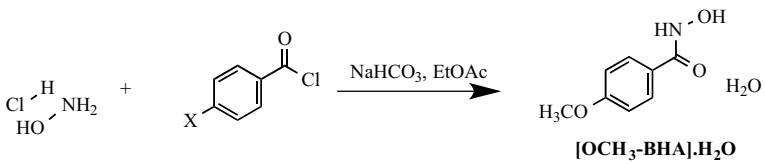

Scheme 3 Formation reaction of Cr(III) complexes of BHA and its derivatives

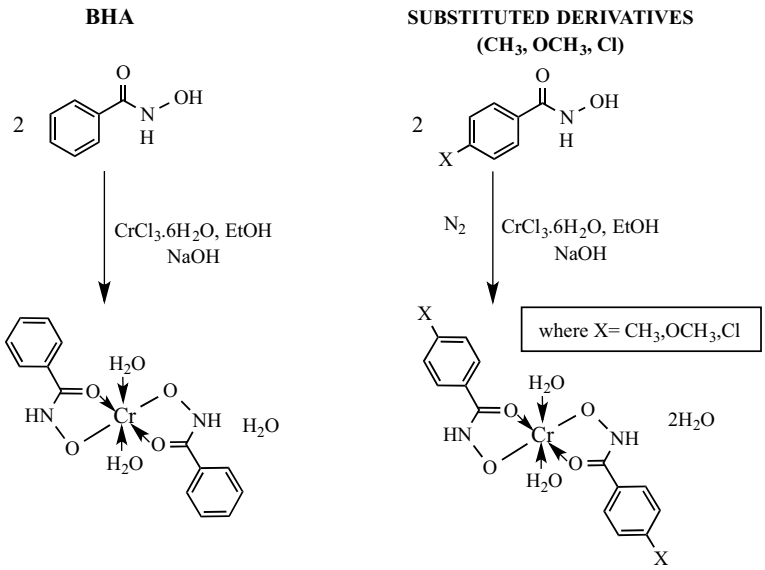

465.20 $[M+H]^+$; Found: 465.22 $[M+H]^+$. Molar conductance (DMSO, Ω^{-1} cm^2 mol^{-1}): 4.06.

iii) **Synthesis of Cr(III) methylbenzohydroxamic acid, $[Cr(CH_3–BHA)_2(H_2O)_2]\cdot 2H_2O$**

Chromium(III) chloride hexahydrate, $CrCl_3\cdot 6H_2O$ (0.6661 g, 5 mmol) was dissolved in 10 mL of hot deionized water. 10 mL of absolute ethanol was used to dissolve CH_3–BHA (1.4356 g, 10 mmol). Then, the mixture was stirred under nitrogen (N_2) gas. The green precipitate was filtered, washed with the warm water and air-dried for 24 h before stored in desiccator. Green solid; yield, 44.13%; m.p. > 250 ºC. Anal. Calcd. for $C_{16}H_{24}N_2O_8Cr$ (424.40 g mol^{-1}): C, 45.29; H, 5.70; N, 6.60; Found: C, 45.52; H, 5.31; N, 6.23. IR (KBr, cm^{-1}): 3216 (N–H), 1648 (C = O), 917 (N–O), 478 (Cr–O). MS (m/z): Calcd for $[Cr(CH_3–BHA)_2(H_2O)_2]\cdot 2H_2O$: 379.30 $[M+H]^+$; Found: 379.28.

$[M+H]^+$. Molar conductance (DMSO, Ω^{-1} cm^2 mol^{-1}): 0.

iv) **Synthesis of Cr(III) methoxybenzohydroxamic acid, $[Cr(OCH_3–BHA)_2(H_2O)_2]\cdot 2H_2O$**

10 mL of hot aqueous $CrCl_3\cdot 6H_2O$ (5 mmol, 0.6661 g) solution was mixed with 10 mL of ethanolic solution of OCH_3–BHA (10 mmol, 1.756 g). The mixture was stirred under N_2 gas for 3 h. Grey precipitate was formed, collected by filtration and washed with the warm water. Finally, the precipitate was stored in a desiccator until the next use. Grey solid; yield, 25.68%; m.p. 102–104 ºC. Anal. Calcd. for $C_{16}H_{24}N_2O_{10}Cr$ (456.40 g mol^{-1}): C, 42.11; H, 5.30; N, 6.14; Found: C, 41.51; H, 5.32; N, 6.10. IR (KBr, cm^{-1}): 3285 (N–H), 1669 (C = O), 917 (N–O), 433 (Cr–O). MS (m/z): Calcd for $[Cr(OCH_3–BHA)_2(H_2O)_2]\cdot 2H_2O$: 457.40 $[M+H]^+$; Found: 457.35 $[M+H]^+$. Molar conductance (DMSO, Ω^{-1} cm^2 mol^{-1}): 0.

Cytotoxicity study

Cell culture

The human colorectal carcinoma cell line, HCT116 (ATCC® CCL-247™), was cultured in the Roswell Park Memorial Institute (RPMI-1640) medium with 25 mM HEPES and L-Glutamine (Biowest) supplemented with 10% heat inactivated fetal bovine serum (FBS) (PAA Laboratories) and 1% penicillin/streptomycin (Sigma Aldrich). The cultures were maintained in a humidified incubator at 37 ºC in an atmosphere of 5% CO_2.

MTT assay

HCT116 cells were plated at 7000 cells per well and were incubated at 37 ºC for 24 h. BHA and its derivatives (CH_3–BHA, OCH_3–BHA, and Cl–BHA) and their Cr(III) metal complexes, all soluble in DMSO, were subjected to DMSO serial dilutions before being added to each well. The cells were treated with the compounds at concentrations ranging between 0.01–100 µM and incubated at 37 ºC for 72 h. The cytotoxicity of the compounds was assessed using the MTT method utilizing 3-(4,5-dimethylthiazol-2-yl)-2,5-diphenyl tetrazolium bromide (MTT or formazan) with minor modifications [18]. Briefly, 50 µL of 0.06 mol/L MTT solution was added to each well and the plates were incubated at 37 ºC for 4 h. All solutions were aspirated and the formazan crystals were dissolved in DMSO. The plate was read at 450 nm. Data generated were used to plot a

dose–response curve from which the concentration of compounds required to kill 50% of the cell population (IC_{50}) was determined.

Alpha-glucosidase inhibitory assay

The effects of BHA and its substituted derivatives on alpha-glucosidase inhibition activity was assessed as described by Elya [19], by using alpha-glucosidase from *Saccharomyces cerevisiae*. The substrate, *p*-nitropheynyl glucopyranoside (*p*NPG) (1 mM) was prepared in 30 mM of potassium phosphate buffer (pH 6.8). 10 µL of tested compounds with different concentrations (0.1–100 mmol/L) was pre-incubated with 10 µL of alpha-glucosidase (0.02 U/mL) at 37 ºC for 10 min. Then, 50 µL of 1 mM *p*NPG was added to the mixture to start the reaction. The reaction was incubated at 37 ºC for another 30 min. Alpha-glucosidase inhibition activity was determined by measuring the yellow colored *para*-nitrophenol at 405 nm released from *p*NPG. IC_{50} of alpha-glucosidase inhibition activity was calculated and determined by using Prism 7.0. IC_{50} data is representing 50% inhibition of enzyme activity towards the concentration of tested compounds. The percent inhibition was calculated using Eq. 1:

$$\%\ \text{Inhibition} = \left(\left(A_c - A_e\right)/Ac\right) * 100$$

where A_c and A_e are the absorbance of the control and extract, respectively.

Molecular docking study

The binding modes between the active complexes and binding sites of alpha-glucosidase have been carried out through molecular docking study using Autodock package [20]. X-ray coordinates of the targeted alpha-glucosidase and the original docked acarbose and glucose ligands were downloaded from the RCSB data bank website with PDB codes 3W37, 3WY2, respectively [17, 21]. The docking steps have been described in our previous studies [22, 23].

Results and discussion

Infrared (IR) spectroscopy

The infrared spectra provide valuable information regarding functional groups attached to the metal. The observable differences of the spectra of the hydroxamic acids and Cr(III) complexes suggesting there is complexation occurred.

For the Cr(III) complexes, the coordination modes suggested is through bidentate *O,O* modes from the IR spectra obtained. The disappearance of the O–H band in the region of 2760–2749 cm^{-1} indicating the deprotonation of OH in the complexes that coordinate through the oxygen atom from hydroxyl groups [24, 25]. The shifting of (C = O) to a lower wavenumber and appeared at 1602 cm^{-1} for BHA series indicating the involvement of carbonyl (C = O) during complexation via oxygen atom [26]. The involvement of C = O during complexation is supported by the appearance of the new weak band, (Cr–O) at a range of 489–433 cm^{-1} for all complexes [27]. The presence of NH in the complexes indicates that NH group is not involved in complexation [28].

For substituted derivatives BHA, there is no appreciable shift for C = O observed throughout the spectra but the bands appeared as a shoulder. This case may be due to the mixing C = C of aryl moiety. The medium bands at 899–917 cm^{-1} in all series can be ascribed as (N–O) where this band does not undergo any change, suggesting that –NO is retained and not coordinated. The difference Δ is less than 200 cm^{-1} indicates that the ligands act as bidentate in all complexes [20], therefore suggesting the coordination of the complexes is through oxygen atoms (*O,O*).

Nuclear magnetic resonance (NMR) spectroscopy

The ^{1}H NMR spectra for the hydroxamic acids were recorded in DMSO-d_6 using tetramethylsilane (TMS) as the internal standard. BHA gave a singlet at 9.08 ppm attributable to N–H proton. Multiplets were observed at 7.41–7.76 ppm indicating the aromatic protons. A singlet was observed at 11.24 ppm indicating the OH proton, appeared downfield because of the deshielding of the electronegative atom, oxygen [29].

For CH_3–BHA, a singlet was observed indicating –CH_3 group at 4.91 ppm. Multiplets were observed at 7.23–7.62 ppm assignable to aromatic protons. Singlets for −OH and −NH groups were not observed due to proton exchange with deuterium in the solvent [30]. For Cl–BHA, singlets were observed at 9.16 ppm for −NH and 11.36 ppm for −OH group. Multiplets were observed at 7.54–7.80 ppm indicating the aromatic protons. For OCH_3–BHA, a singlet for −OCH_3 group was observed at 3.80 ppm [31]. The aromatic protons peaks were observed at 6.99–7.74 ppm as a doublet. −OH and −NH group peaks were observed as a singlet at 8.93 and 11.11 ppm, respectively.

For ^{13}C NMR, there are two types of important carbons, i.e., carbonyl and aromatic. The carbonyl carbons appeared downfield at 164.79, 164.03, 163.14 and 161.43 ppm for BHA, CH_3–BHA, Cl–BHA, and OCH_3–BHA, respectively. These carbonyl carbons appeared downfield because of the deshielding effect of an electronegative element, nitrogen [32]. Aromatic carbons of BHA appeared at 127.32–133.21 ppm, Cl–BHA appeared at 128.43–135.91 ppm, CH_3–BHA, the peaks appeared at 126.73–140.61 ppm, and for OCH_3–BHA, the aromatic

carbons appeared at 113.55–131.29 ppm. The methyl peak for CH_3–BHA appeared at 20.89 ppm and the methoxy peak for OCH_3–BHA appeared at 55.20 ppm [33]. Unfortunately, ^{1}H and ^{13}C NMR for Cr(III) complexes could not be obtained because all complexes are paramagnetic [34].

Thermogravimetric analysis (TGA)

The summary of the thermal decomposition behavior of all Cr(III) complex through thermogravimetric analysis (TGA) is presented in Table 1. All Cr(III) complexes, unsubstituted and substituted, displayed decomposition of 1 and 2 non-coordinated water molecules, respectively, at the temperature range of 25–100 ºC [34], then the thermal decomposition continued with the removal of two coordinated water molecules each in the range of 100–220 ºC (Table 2).

The unsubstituted complex $[Cr(BHA)_2(H_2O)_2]\bullet H_2O$ then further decomposed to lose 33% of the mass up to 600 ºC due to the loss of two C_5H_5 fragments of the benzene rings. The weight percent remained constant at 52% beyond 600 °C up to 900 ºC, attributed to the central $CrC_4H_2N_2O_4$ moiety (Fig. 1a). $[Cr(Cl–BHA)_2(H_2O)_2]\bullet 2H_2O$ lost 66% of the mass at 172–284 ºC due to the departure of $2(C_7H_4Cl)$ moieties followed by the removal of 2NH fragments (9%) at 284–469 ºC. Beyond 469 ºC, only the oxide of chromium was left, with no further decomposition (Fig. 1b). The complex $[Cr(CH_3-BHA)_2(H_2O)_2]\bullet 2H_2O$ lost 48.89% at 172–380 due to the departure of $2(C_8H_7)$ moieties, beyond which a slow incomplete decomposition occurred up to the final recorded temperature of 900 °C, leaving the central $CrO_4N_2H_2$ (Fig. 1c).$[Cr(OCH_3-BHA)_2(H_2O)_2]\cdot 2H_2O$ lost 46.32% at 202–600 due to the departure of $2(C_7H_7O)$ moieties leaving behind the central moiety $CrC_2H_2N_2O_4$ (Fig. 1d) that remained up to 900 °C.

Mass spectroscopy and molar conductivity

The mass spectroscopy of all ligands and Cr(III) complexes showed good agreement between the calculated and experimental molar masses, in parallel with the good match between the calculated and experimental percentages of C, H and N. The low molar conductivity values of the metal

Table 1 Thermal behaviour indicating the loss of H_2O molecules from all Cr(III) complexes

Compound	Temperature range (°C)	Weight loss (%) found (calculated)	Lost species
$[Cr(BHA)_2(H_2O)_2]\cdot H_2O$	40–100	5.00 (4.76)	- 1 non-coordinated H_2O
	150–220	10.00 (9.52)	- 2 coordinated H_2O
	220–600	33.00 (34.36)	- $2(C_5H_5)$
$[Cr(Cl\text{-}BHA)_2(H_2O)_2]\ 2H_2O$	25–100	7.00 (7.74)	- 2 non-coordinated H_2O
	100–172	8.00 (7.74)	- 2 coordinated H_2O
	172–284	66.00 (65.29)	-$2(C_7H_4Cl)$
	284–469	9.00 (7.93)	-2(NH)
$[Cr(CH_3\text{-}BHA)_2(H_2O)_2]\cdot 2H_2O$	54–100	8.89 (8.48)	- 2 non-coordinated H_2O
	107–172	8.89 (8.48)	- 2 coordinated H_2O
	172–380	48.89 (48.54)	-$2(C_8H_7)$
$[Cr(OCH_3\text{-}BHA)_2(H_2O)_2]\cdot 2H_2O$	57–100	7.75 (7.89)	- 2 non-coordinated H_2O
	107–202	7.95 (7.89)	- 2 coordinated H_2O
	202–600	46.32 (46.89)	-$2(C_7H_7O)$

Table 2 Electronic transitions of hydroxamic acids and their Cr(III) complexes

Ligand/complex	$\pi \rightarrow \pi^*$(aromatic) (nm)	$n \rightarrow \pi^*(C=O)$ (nm)	Ligand-to-metal charge transfer (LMCT)
BHA	220	336	–
$[Cr(BHA)_2(H_2O)_2]\cdot H_2O$	227	275	–
Cl–BHA	240	–	–
$[Cr(Cl–BHA)_2(H_2O)_2]\cdot 2H_2O$	237	326	–
CH_3–BHA	236	–	–
$[Cr(CH_3–BHA)_2(H_2O)_2]\cdot 2H_2O$	238	312	467
$[OCH_3\text{-}BHA]\cdot H_2O$	254	–	–
$[Cr(OCH_3\text{-}BHA)_2(H_2O)_2]\cdot 2H_2O$	254	–	–

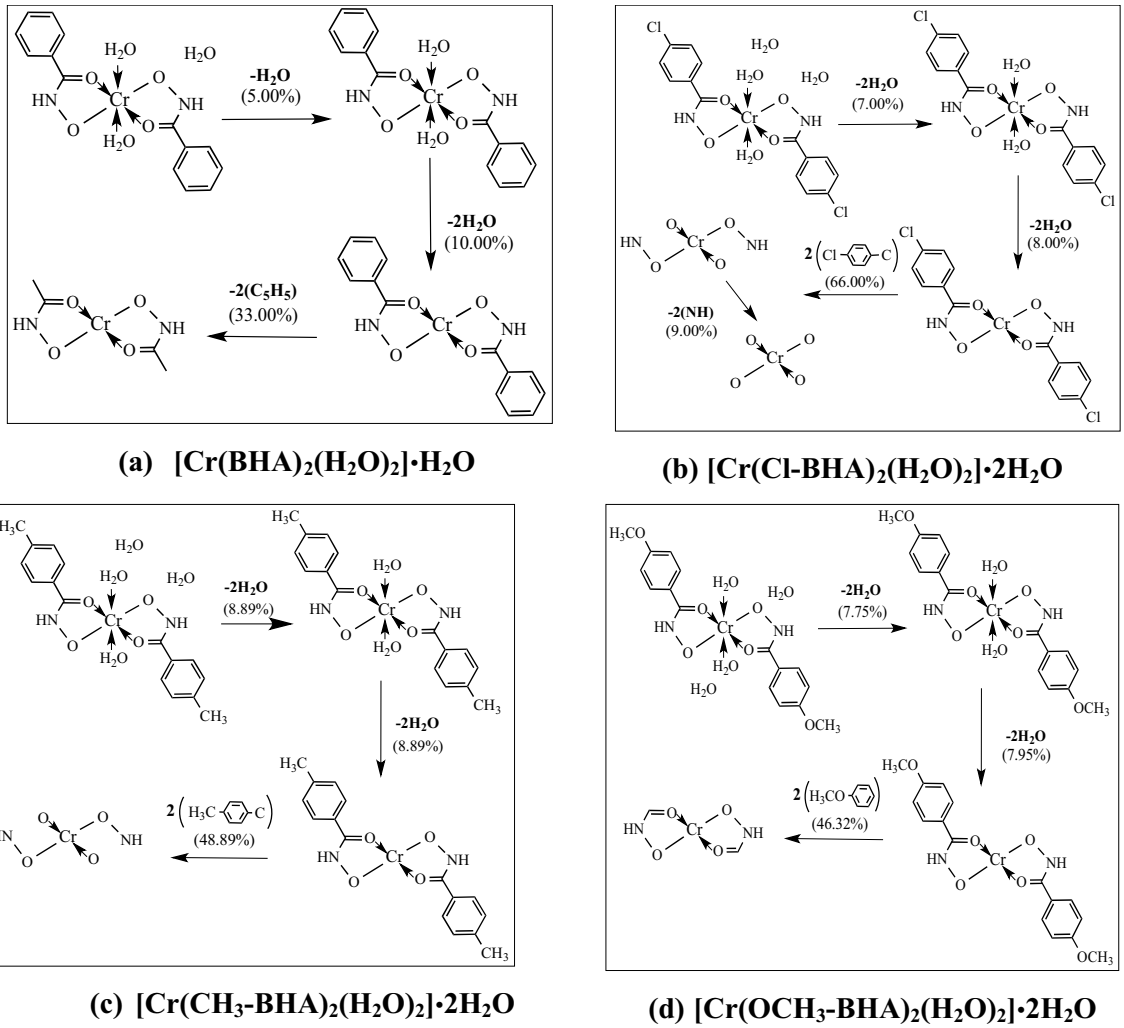

Fig. 1 Thermal decomposition of Cr(III) complexes

complexes as solutions in DMSO indicated the non-electrolytic behavior, i.e., the non-existence of free ions acting as electrolytes in the solution [35].

UV–visible spectroscopy

The UV–Visible spectra of hydroxamic acids and their corresponding Cr(III) complexes as ethanolic solutions at concentrations of 1.00×10^{-4} and 1.00×10^{-5} M were measured in the range of 200–800 nm (Table 2). The π–π^*(aromatic) and n–π^*(C = O) electronic transitions of each compound were identified in the regions of 220–254 and 275–336 nm, respectively. The $n \rightarrow \pi^*$(C = O) peaks of the substituted ligands and the $[Cr(OCH_3–BHA)_2(H_2O)_2]\cdot 2H_2O$ complex were not observed, likely due to the presence of hydrogen bonding between the polar solvent and the chromophore [36] or obscured by the strong neighboring peak.

Table 3 IC_{50} values of BHA, its substituted derivatives and Cr(III) complexes on HCT116 cells

Ligand/complex	$IC_{50} \pm$ SEM (μM)
BHA	> 100
$[Cr(BHA)_2(H_2O)_2]\cdot H_2O$	> 100
Cl-BHA	58.33 ± 1.87
$[Cr(Cl–BHA)_2(H_2O)_2]\cdot 2H_2O$	27.50 ± 5.09
CH_3–BHA	> 100
$[Cr(CH_3–BHA)_2(H_2O)_2]\cdot 2H_2O$	> 100
$[OCH_3–BHA]\cdot H_2O$	38.00 ± 4.82
$[Cr(OCH_3–BHA)_2(H_2O)_2]\cdot 2H_2O$	20.56 ± 2.47
5-Fluorouracil (standard)	13.07 ± 0.00

Comparing the spectra of BHA and $[Cr(BHA)_2(H_2O)_2]\cdot H_2O$, the $n \rightarrow \pi^*$(C = O) was observed to experience a hypsochromic shift towards a lower

wavelength, from 336 to 275 nm, indicating that complexation has occurred [37]. The $\pi \rightarrow \pi^*$(aromatic) did not show any significant shifting upon complexation indicating that donor atoms involved in bonding with Cr(III) centers were not in the proximity of the aromatic moieties, hence supporting the proposed structure of Cr(III) coordination through C = O, located two atoms away from the benzene ring. The ligand-to-metal charge transfer (LMCT) bands were only observed in $[Cr(CH_3–BHA)_2(H_2O)_2]\bullet 2H_2O$ at 467 nm [34].

Cytotoxicity assay

The synthesized hydroxamic acids and Cr(III) complexes were evaluated for cytotoxicity against human colorectal carcinoma cell line, HCT116. All tested compounds induced a concentration-dependent anti-proliferative effect towards HCT116 cells upon treatment for 24 h [38]. IC_{50} values of all compounds on HCT116 cells are shown in Table 3.

BHA, CH_3–BHA and their Cr(III) complexes displayed very low cytotoxicity against HCT116. The OCH_3– and Cl– substituted ligands and complexes showed much enhanced antiproliferative properties with IC_{50} values of 20.56–58.33 µM with $[Cr(OCH_3–BHA)_2(H_2O)_2]\bullet 2H_2O$ being the most active. The presence of lone pair bearing OCH_3 and Cl substituents enhanced the activity, particularly in the presence of Cr(III) centers.

The Cr(III) complexes revealed higher cytotoxicity than their parent ligands. This observation can be explained through Tweedy's chelation theory and Overtone's cell permeability rule. According to Tweedy, the polarity of the metal ion will be lowered upon complexation due to the overlapping of ligand orbitals and partial sharing of positive charge with the donor groups. Complexation also increases the delocalization of π-electrons over the entire chelate ring, enhancing the lipophilicity of the complexes. Overtone's concept of cell permeability states that the entry of any molecule into a cell is governed by its lipophilicity because the lipid membrane surrounding the cell favors the passage of materials that are soluble in lipids. Thus, the increased lipophilicity upon complexation enhances the penetration of the complexes into the cells and blocks the metal binding sites of receptors [39].

Table 4 Alpha-glucosidase inhibitory activity against BHA and its substituted derivatives of CH_3-BHA, OCH_3-BHA, Cl-BHA series

Ligand/complex	$IC_{50} \pm$ SEM (µM)
Acarbose (standard)	418 ± 0.55
BHA	Not active
$[Cr(BHA)_2(H_2O)_2]\cdot H_2O$	28.7 ± 0.98
Cl–BHA	Not active
$[Cr(Cl–BHA)_2(H_2O)_2]\cdot 2H_2O$	169.5 ± 0.46
CH_3–BHA	Not active
$[Cr(CH_3–BHA)_2(H_2O)_2]\cdot 2H_2O$	69.28 ± 0.13
$[OCH_3–BHA]\cdot H_2O$	Not active
$[Cr(OCH_3–BHA)_2(H_2O)_2]\cdot 2H_2O$	355.9 ± 0.87

Alpha-glucosidase inhibitory activity and molecular docking results

All of the synthesized ligands and complexes were tested on their alpha-glucosidase inhibitory activity against *Saccharomyces cerevisiae* (Table 4). At 100 µM, all hydroxamic acids are inactive, whereas all Cr(III) complexes showed excellent inhibitory properties with IC_{50} values much lower than the Acarbose standard. The highest inhibition towards alpha-glucosidase was shown by $[Cr(BHA)_2(H_2O)_2]\cdot H_2O$ followed by $[Cr(CH_3–BHA)_2(H_2O)_2]\cdot 2H_2O$, $[Cr(Cl–BHA)_2(H_2O)_2]\cdot 2H_2O$ and $[Cr(OCH_3–BHA)_2(H_2O)_2]\cdot 2H_2O$ with the IC_{50} values of 28.7, 69.28, 169.5 and 355.9 µM, respectively. It was interesting to note that in the presence of substituents lowered the alpha-glucosidase inhibition, in contrast to the antiproliferative properties.

In an attempt to rationalize the observed alpha-glucosidase inhibition of the active complexes, binding energies of the stable complexes formed between docked ligands and alpha-glucosidase, the number of intermolecular hydrogen bonds between the docked ligands and residues into the active site in alpha-glucosidase; and the number of residues involved in intermolecular interactions are gathered in Table 5.

As can be seen from Table 5, all complexes formed between the docked metal complexes $[Cr(BHA)_2(H_2O)_2]\cdot H_2O$, $[Cr(CH_3–BHA)_2(H_2O)_2]\cdot 2H_2O$, $[Cr(OCH_3–BHA)_2(H_2O)_2]\cdot 2H_2O$ and $[Cr(Cl–BHA)_2(H_2O)_2]\cdot 2H_2O$ into the active site of the targeted enzyme showed negative binding energies, which

Table 5 Docking binding energies and the inhibition activities of the docked Cr(III) complexes into the active site of alpha-glucosidase (PDB 3W37)

Complexes	Free binding energy (kcal/mol)	Number of HBs	Number of closest residues	$IC_{50} \pm$ SEM
$[Cr(BHA)_2(H_2O)_2]\cdot H_2O$	− 8.78	5	9	28.7 ± 0.98
$[Cr(Cl–BHA)_2(H_2O)_2]\cdot 2H_2O$	− 7.66	4	11	169.5 ± 0.46
$[Cr(CH_3–BHA)_2(H_2O)_2]\cdot 2H_2O$	− 7.81	5	11	69.28 ± 0.13
$[Cr(OCH_3\text{-}BHA)_2(H_2O)_2]\cdot 2H_2O$	− 7.75	6	10	355.9 ± 0.87

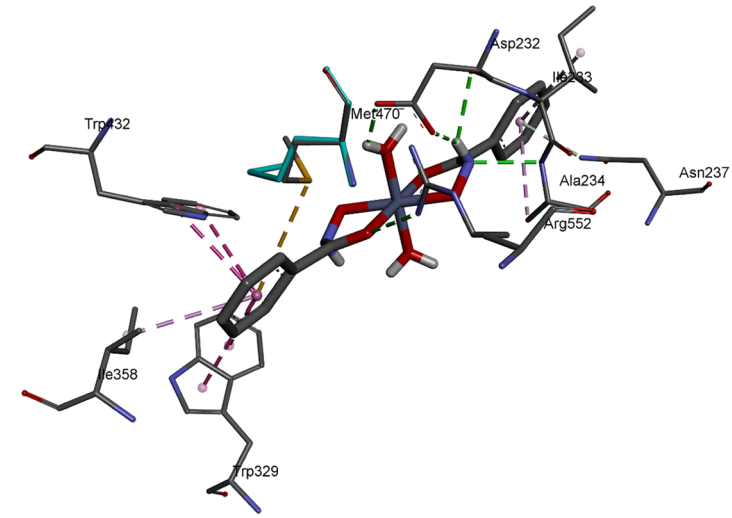

$[Cr(BHA)_2(H_2O)_2]\cdot H_2O$

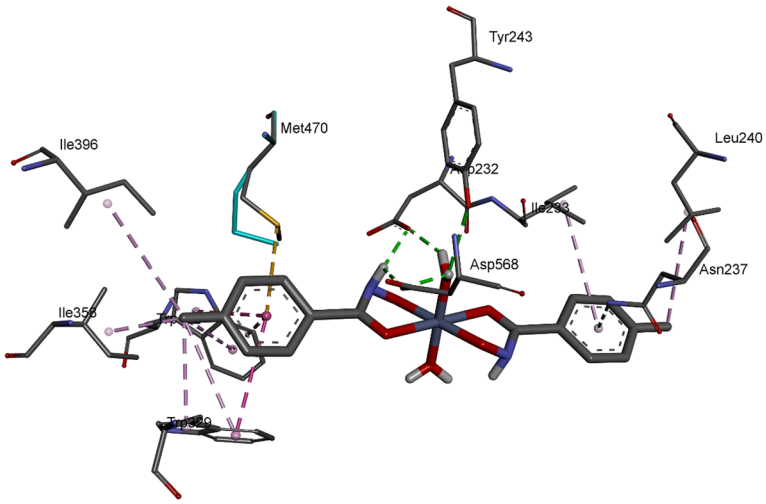

$[Cr(CH_3\text{-}BHA)_2(H_2O)_2]\cdot 2H_2O$

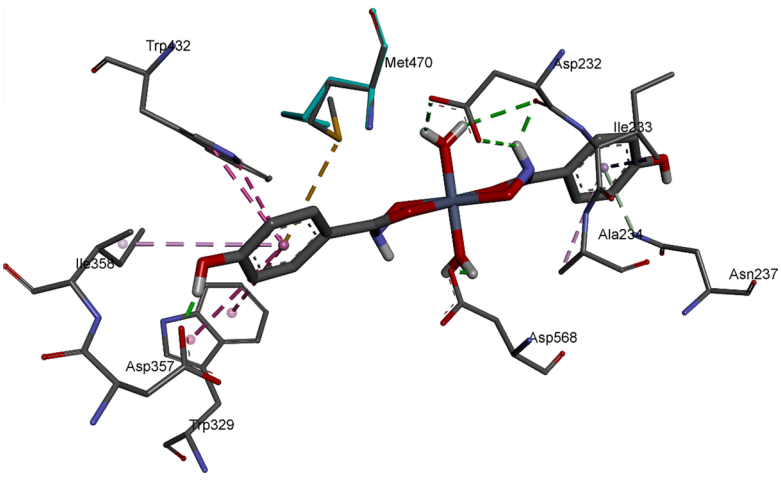

$[Cr(OCH_3\text{-}BHA)_2(H_2O)_2]\cdot 2H_2O$

Fig. 2 3D views of molecular interactions between active site residues of alpha-glucosidase and the docked complexes

Fig. 2 (continued)

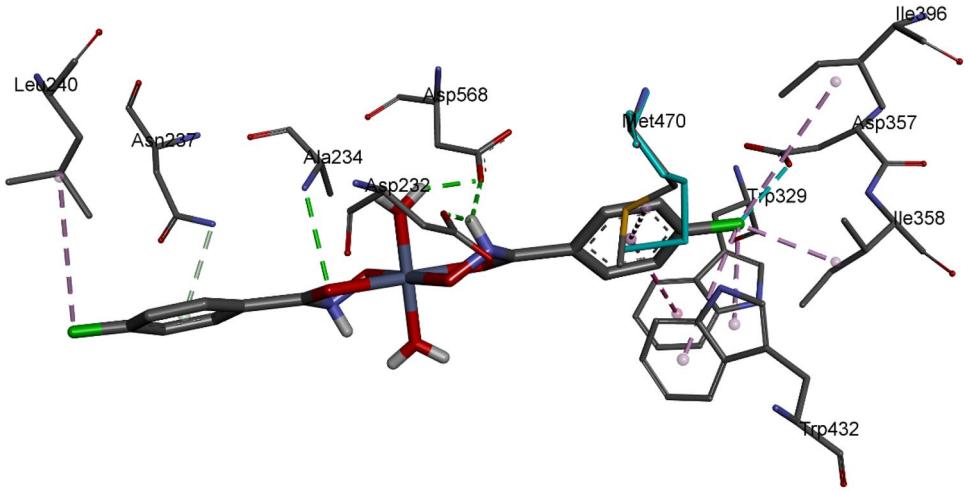

$[Cr(Cl\text{-}BHA)_2(H_2O)_2]\cdot 2H_2O$

indicates that the docking of the title complexes are thermodynamically favorable. Experimental tests showed that $[Cr(BHA)_2(H_2O)_2]\cdot H_2O$ is more active than the Cr complexed substituted ligand $[Cr(CH_3\text{–}BHA)_2(H_2O)_2]\cdot 2H_2O$, $[Cr(OCH_3\text{–}BHA)_2(H_2O)_2]\cdot 2H_2O$ and $[Cr(Cl\text{–}BHA)_2(H_2O)_2]\cdot 2H_2O$ (Table 4). This result is in good accordance with the docking results, which showed that the docked alpha-glucosidase–Cr(CH_3O–BHA) Cr(BHA) complex is the most stable complex with a binding energy of − 8.78 kcal/mol. Similarly, the higher inhibition efficiency of $[Cr(CH_3\text{–}BHA)_2(H_2O)_2]\cdot 2H_2O$ compared with $[Cr(OCH_3\text{–}BHA)_2(H_2O)_2]\cdot 2H_2O$ and $[Cr(Cl\text{–}BHA)_2(H_2O)_2]\cdot 2H_2O$ is mainly refer to the stability of the complex formed with the former compared with the latters (Table 5). It is worth to mention that the most active complexes established five hydrogen bonds with active amino acids of alpha-glucosidase. In case of alpha-glucosidase–Cr(BHA) complex, the strongest hydrogen bond is formed between ASP232 amino acid and the hydrogen atom of water in $[Cr(BHA)_2(H_2O)_2]\bullet H_2O$ of 2.06 Å, while for alpha-glucosidase–$[Cr(CH_3BHA)_2(H_2O)_2]$ the strongest hydrogen bond is established between ASP568 amino acid and the hydrogen atom of water in $[Cr(CH_3\text{–}BHA)_2(H_2O)_2]\bullet 2H_2O$ of 2.15 Å (Figs. 2, 3). It is obvious from docking results (Table 5 and Figs. 2, 3) that the number of the closest residues involved in intermolecular interactions with docked complexes has a negligible effect on alpha-glucosidase.

From the docking results, it is obvious that the presence of electron-donating or withdrawing groups had no significant effects on the inhibitory activity of alpha-glucosidase, in total accord to the experimental findings. All the chromium complexes have greater potential as alpha-glucosidase inhibitors, seen through better suppression of the enzyme compared to the standard, Acarbose. Chromium complexes undergo hydrogen bondings to the enzyme and its substrates as shown in Fig. 2, and the conformation and orientation of the inhibitors at the active site make them better in inhibiting the alpha-glucosidase [31].

Conclusion

BHA and its substituted derivatives together with Cr(III) complexes were successfully synthesized and characterized by elemental analysis, FTIR, ^{1}H and ^{13}C NMR, UV–Visible, TGA analysis, mass spectroscopy as well as molar conductivity. All the spectral data showed that the complexation of the metal center, Cr(III) to the ligands is through oxygen and oxygen atoms (*O,O*) in a bidentate manner. On the basis of chelation theory, metal complexes showed better toxicity than free ligands.$[OCH_3\text{–}BHA]\cdot H_2O$ and its Cr(III) complex showed the highest inhibition towards the HCT116 albeit less potent than the 5-FU standard. $[Cr(BHA)_2(H_2O)_2]\cdot H_2O$, $[Cr(CH_3\text{–}BHA)_2(H_2O)_2]\cdot 2H_2O$, $[Cr(OCH_3\text{–}BHA)_2(H_2O)_2]\cdot 2H_2O$ and $[Cr(Cl\text{–}BHA)_2(H_2O)_2]\cdot 2H_2O$ showed better alpha-glucosidase inhibition ability than the Acarbose standard. Binding energy analysis of complexes formed between the active complexes and amino acids residues of alpha-glucosidase revealed the docking of the complexes is thermodynamically favorable, and the higher inhibition efficiency of $[Cr(BHA)_2(H_2O)_2]\cdot H_2O$ is mainly due to its stability and binding energy.

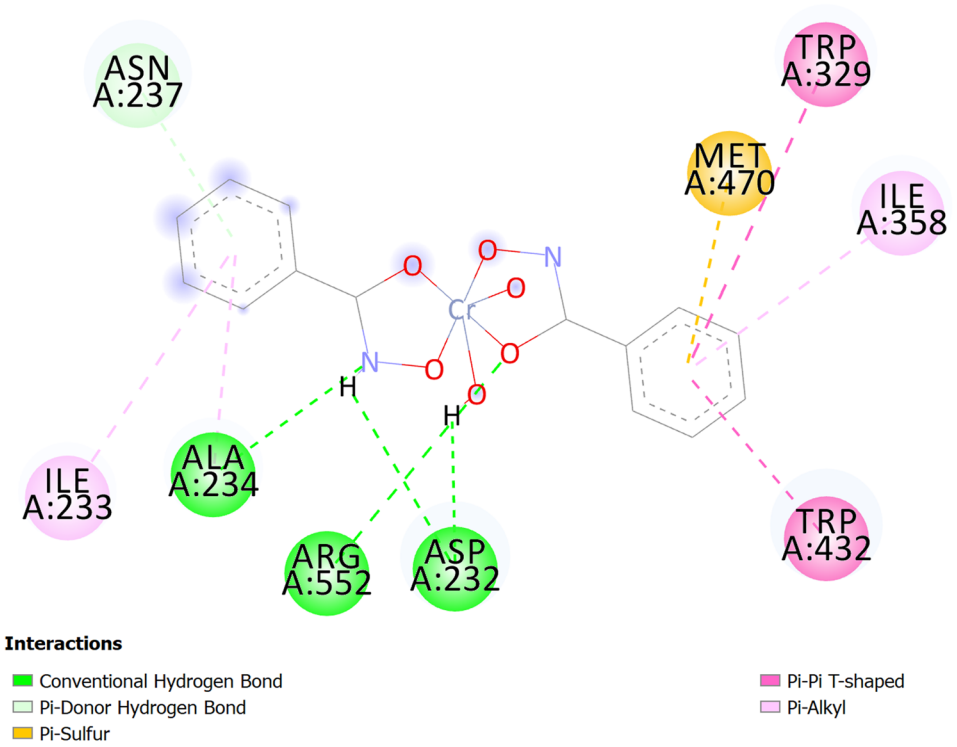

$[Cr(BHA)_2(H_2O)_2]\cdot H_2O$

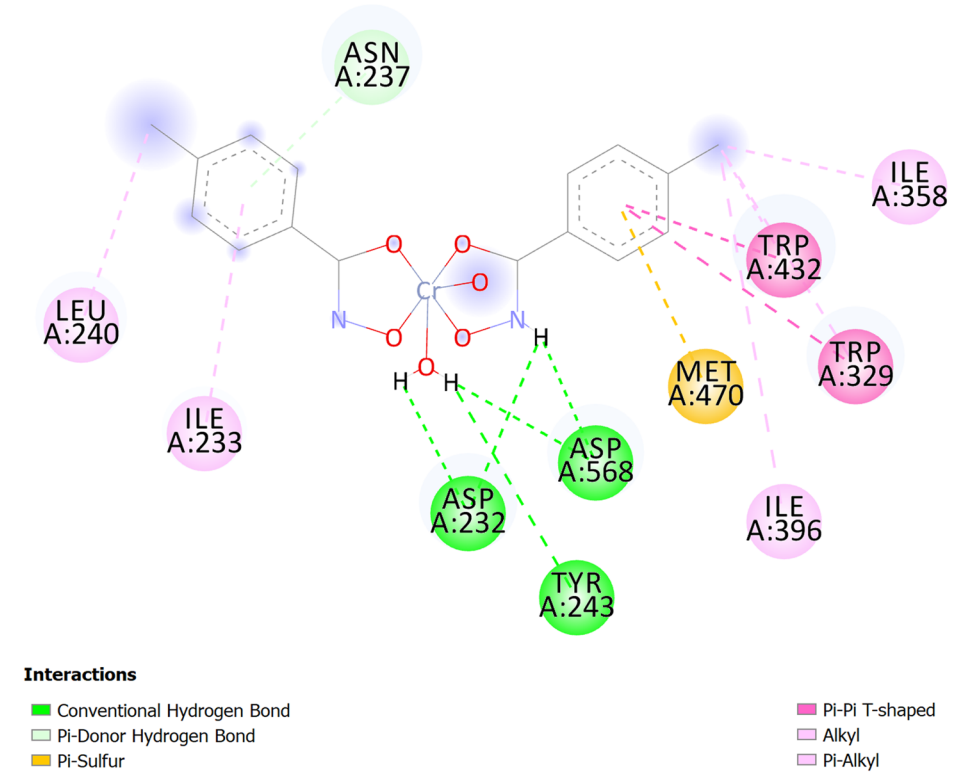

Fig. 3 2D views of molecular interactions between active site residues of alpha-glucosidase and the docked Cr(III) complexes

Fig. 3 (continued)

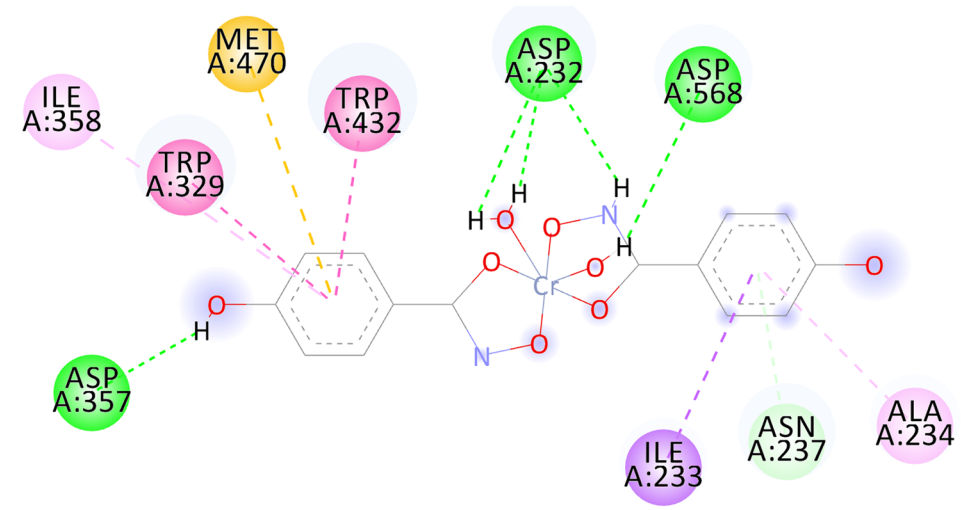

$[Cr(OCH_3\text{-}BHA)_2(H_2O)_2]\cdot 2H_2O$

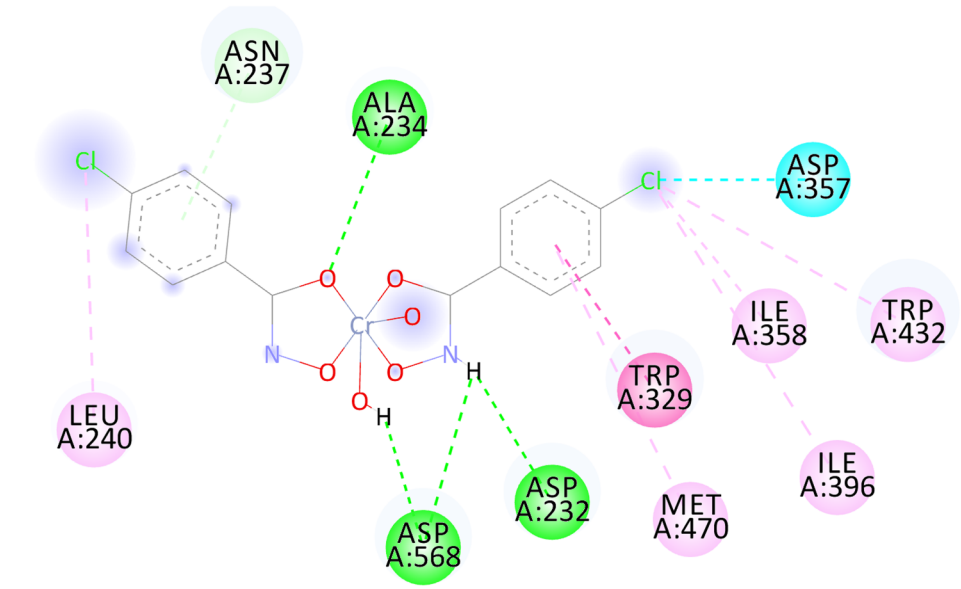

$[Cr(Cl\text{-}BHA)_2(H_2O)_2]\cdot 2H_2O$

Funding This work was funded by the Ministry of Higher Education of Malaysia for the research fund; 600-IRMI 5/3/GIP (004/2018), Universiti Teknologi MARA and AuRIns for research facilities and Faculty of Pharmacy for the facilities on cytotoxicity study.

Compliance with ethical standards

Conflict of interest The authors declare that they have no conflict of interest.

References

1. Griffith D, Lyssenko K, Jensen P, Kruger PE, Marmion CJ (2005) Novel platinum(II) ammine hydroxamate and hydroximate complexes and the platinum-assisted hydrolysis of hydroxamic acids. Dalton Trans 5:956–961
2. Dixon NE, Hinds JA, Fihelly AK, Gazzola C, Winzor DJ, Blakeley RL, Zerner B (1980) Jack bean urease (EC 3.5.1.5). IV. The molecular size and the mechanism of inhibition by hydroxamic acids. Spectrophotometric titration of enzymes with reversible inhibitors. Can J Biochem 58:1323–1334
3. Wilkes SH, Prescott JM (1987) Hydroxamate-induced spectral perturbations of cobalt Aeromonas Aminopeptidase. J Biol Chem 262(18):8621–8625
4. Baker JO, Wilkes SH, Bayliss ME, Prescott JM (1983) Hydroxamates and aliphatic boronic acids: marker inhibitors for Aminopeptidase. Biochemistry 22(9):2098–2103
5. Sharma N, Kumari M, Kumar V, Chaudhry S, Kanwar S (2010) Synthesis, characterization, and antibacterial activity of vanadium(IV) complexes of hydroxamic acids. J Coord Chem 63:176–184
6. Griffith D, Bergamo A, Pin S, Vadori M, Muller-Bunz H, Sava G, Marmion CJ (2007) Novel platinum pyridinehydroxamic acid complexes: synthesis, characterisation, X-ray crystallographic study and nitric oxide related properties. Polyhedron 26:4697–4706
7. Marmion CJ, Murphy T, Docherty JR, Nolan KB (2000) Hydroxamic acids are nitric oxide donors. Facile formation of ruthenium(II)-nitrosyls and NO-mediated activation of guanylate cyclase by hydroxamic acids. ChemComm 13:1153–1154
8. Wang WH, Liu WS, Wang YW, Li Y, Zheng LF, Wang DQ (2007) Self-assembly and cytotoxicity study of waterwheel-like dinuclear metal complexes: The first metal complexes appended with multiple free hydroxamic acid groups. J Inorg Biochem 101(2):297–304
9. García B, Ibeas S, Leal JM, Secco F, Venturini M, Senent ML, Alfonso N, Muñoz C (2005) Conformations, protonation sites, and metal complexation of benzohydroxamic acid A theoretical and experimental study. Inorg Chem 44(8):2908–2919
10. Adiguzel E, Yilmaz F, Emirik M, Ozil M (2017) Synthesis and characterization of two new hydroxamic acids derivatives and their metal complexes. An investigation on the keto/enol, E/Z and hydroxamate/hydroximate forms. J Mol Struct 1127:403–412
11. Cefalu TW, Hu FB (2004) Role of chromium in human health and in diabetes. Diabetes Care 27(11):2741–2751
12. Vincent JB (2001) The bioinorganic chemistry of chromium(III). Polyhedron 20:1–26
13. Dong J, Liu B, Liang G, Yang B (2018) Synthesis, biological activity and toxicity of chromium(III) metformin complex as potential insulin-mimetic agent in C57BL/6 mice. J Coord Chem 71(10):1526–1541
14. Król E, Krejpcio Z, Okulicz M, Śmigielska H (2019) Chromium(III) glycinate complex supplementation improves the blood glucose level and attenuates the tissular copper to zinc ratio in rats with mild hyperglycaemia. Biol Trace Elem Res 193:185–194
15. Jacewicz D, Siedlecka-Kroplewska K, Pranczk J, Wyrzykowski D, Woźniak M, Chmurzyński L (2014) *Cis*-$[Cr(C_2O_4)(pm)(OH_2)_2]^+$ coordination ion as a specific sensing ion for H_2O_2 detection in HT22 cells. Molecules 19(6):8533–8543
16. Rahman N, Muhammad I, Nayab GE, Khan H, Aschner M, Filosa R, Daglia M (2019) Molecular docking of isolated alkaloids for possible α-glucosidase inhibition. Biomolecules 9(10):1–17
17. Tagami T, Yamashita K, Okuyama M, Mori H, Yao M, Kimura A (2013) Molecular basis for the recognition of long-chain substrates by plant alpha-glucosidases. J Biol Chem 288:19296–19303
18. Hazalin NA, Ramasamy K, Lim SSM, Wahab IA, Cole AL, Majeed ABA (2009) Cytotoxic and antibacterial activities of endophytic fungi isolated from plants at the National Park, Pahang, Malaysia. BMC Complement Altern Med 9:1–5
19. Elya B, Basah K, Mun'im A, Yuliastuti W, Bangun A, Septiana EK, Iinuma M (2011) Screening of-glucosidase inhibitory activity from some plants of Apocynaceae, Clusiaceae, Euphorbiaceae, and Rubiaceae. J Biomed Biotechnol 2012:1–7
20. Morris GM, Huey R, Lindstrom W, Sanner MF, Belew RK, Goodsell DS, Olson AJ (2009) AutoDock4 and AutoDockTools4: automated docking with selective receptor flexibility. J Theor Comput 30:2785–2791
21. Shen X, Saburi W, Gai Z, Kato K, Ojima-Kato T, Yu J, Komoda K, Kido Y, Matsui H, Mori H (2015) Structural analysis of the α-glucosidase HaG provides new insights into substrate specificity and catalytic mechanism. Acta Crystallogr D 71:1382–1391
22. Al-Salahi R, Ahmad R, Anouar E, Iwana nor Azman N I, Marzouk M, Abuelizz H A, (2018) 3-Benzyl (phenethyl)-2-thioxobenzo [g] quinazolines as a new class of potent α-glucosidase inhibitors: synthesis and molecular docking study. Future Med Chem 10:1889–1905
23. Abuelizz HA, Dib RE, Marzouk M, Anouar E-H, Maklad AY, Attia NH, Al-Salahi R (2017) Molecular docking and anticonvulsant activity of newly synthesized quinazoline derivatives. Molecules 22:1094
24. Griffith D, Krot K, Comiskey J, Nolan KB, Marmion CJ (2008) Monohydroxamic acids and bridging dihydroxamic acids as chelators to ruthenium(III) and as nitric oxide donors: syntheses, speciation studies and nitric oxide releasing investigation. Dalton Trans 1:137–147
25. Obrien EC, Le Roy S, Levaillain J, Fitzgerald DJ, Nolan KB (1997) Metal complexes of salicylhydroxamic acid and O-acetylsalicylhydroxamic acid. Inorg Chim Acta 266:117–120
26. Farkas E, Enyedy EA, Micera G, Garribba E (2000) Coordination modes of hydroxamic acids in copper(II), nickel(II) and zinc(II) mixed-ligand complexes in aqueous solution. Polyhedron 19:1727–1736
27. Fazary AE (2014) Metal complexes of salicylhydroxamic acid and 1, 10-phen-anthroline; equilibrium and antimicrobial activity studies. Bull Chem Soc Ethiop 28:393–402
28. Shotor S, Kassim K, Bahron H, Tajuddin A, Yusof F, Marmion C, Rajab NF (2010) In-vitro cytotoxicity studies of vanadyl complexes with hydroxamic acid series, Science and Social Research (CSSR). In: 2010 international conference on, IEEE, pp 1283–1286
29. Abdualbasit G, Yang F, Emad Y, Mohamed K (2018) Synthesis and characterization of some diorganotin(iv) complexes of *N*-Tolyl- m-nitrobenzohydroxamic acid. J Eng Appl Sci 3:47–50
30. Haratake M, Fukunaga M, Ono M, Nakayama M (2005) Synthesis of vanadium (IV, V) hydroxamic acid complexes and in vivo assessment of their insulin-like activity. J Biol Inorg Chem 10:250–258
31. Deepak Sonu C, Krishna KV, Sapana G (2017) Synthesis, characterization and antimicrobial studies on some pyridoxylidenesulphamethoxazole schiff base tellurium (IV) complexes. Der Pharma Chem 9:59–64
32. Sharma R, Sharma N (2012) Thermal studies of some biologically active oxovanadium (IV) complexes containing 8-hydroxyquinolinate and hydroxamate ligands. J Therm Anal Calorim 110:539–543
33. Temel H, Şekerci M (2001) Novel complexes of manganese (III), cobalt (II), copper (II), and zinc (II) with schiff base derived from 1, 2-bis (p-amino-phenoxy) ethane and salicylaldehyde. Synth React Inorg Met 31:849–857
34. Bakar S N A, Bahron H, Kassim K, Synthesis and characterization of a novel Schiff base derived from 2, 4,

6-trimethyl-m-phenylenediamine with o-vanillin and its metal complexes, Science and Social Research (CSSR). In: 2010 international conference on, IEEE, 2010, pp 463–466.
35. Carrano CJ, Nunn CM, Quan R, Bonadies JA, Pecoraro VL (1990) Monomeric and dimeric vanadium(IV) and-(V) complexes of N-(hydroxyalkyl) salicylideneamines: structures, magnetochemistry and reactivity. Inorg Chem 29:944–951
36. Przychodzen W, Nycz JE, Nam Y-J, Lee D-U (2013) Cytotoxic and antioxidant activities of benzohydroxamic acid analogues. Notes 34:3099
37. Erdener Çıralı D, Uyar Z, Koyuncu İ, Hacıoğlu N (2015) Synthesis, characterization and catalytic, cytotoxic and antimicrobial activities of two novel cyclotriphosphazene-based multisite ligands and their Ru (II) complexes. Appl Organomet Chem 29:536–542
38. Refat MS, El-Korashy SA, Kumar DN, Ahmed AS (2008) Syntheses and characterization of Ru (III) with chelating containing ONNO donor quadridentate schiff bases. Spectrochim. Acta A 70:898–906
39. Indrianingsih AW, Tachibana S, Itoh K (2015) In vitro evaluation of antioxidant and α-Glucosidase inhibitory assay of several tropical and subtropical plants. Procedia Environ Sci 28:639–648